Quantum oscillation of magnetoresistance in tunneling junctions with a nonmagnetic spacer

H. Itoh,[1] J. Inoue,[1,2] A. Umerski,[3] and J. Mathon[4]
[1]*Department of Applied Physics, Nagoya University, Nagoya 464-8603, Japan*
[2]*CREST, JST (Japan Science and Technology), Shibuya-ku, Tokyo 150-0002, Japan*
[3]*Department of Applied Mathematics, Open University, Milton Keynes MK7 6AA, United Kingdom*
[4]*Department of Mathematics, City University, London EC1V 0HB, United Kingdom*
(Received 1 July 2003; published 19 November 2003)

We make a theoretical study of the quantum oscillations of the tunneling magnetoresistance (TMR) as a function of the spacer layer thickness. Such oscillations were recently observed in tunneling junctions with a nonmagnetic metallic spacer at the barrier-electrode interface. We calculate the TMR ratio for disordered tunneling junctions containing a spacer at which quantum well states are formed. A single-orbital tight-binding model, the linear response theory, and the coherent potential approximation are used for the calculation. As a function of the spacer thickness, calculated TMR ratio shows damped oscillation around zero with a single period given by the Fermi wave vector of the spacer, which is consistent with observed results. It is shown that momentum selection due to the insulating barrier and conduction via quantum well states in the spacer, mediated by diffusive scattering caused by disorder, are essential features required to explain the observed oscillation in the TMR ratio. We further show that calculated results can be reproduced by the stationary phase approximation, which implies that obtained results hold qualitatively in more realistic band models.

DOI: 10.1103/PhysRevB.68.174421 PACS number(s): 75.47.De, 73.40.Gk

I. INTRODUCTION

Large magnetoresistance[1,2] observed in ferromagnetic tunneling junctions, ferromagnetic metal (FM)/insulator (I)/FM, currently attracts much interest due to technological applications such as magnetic sensors and magnetic random access memory elements. The tunneling current through FM/I/FM junctions is usually discussed in terms of the spin-polarized densities of states (DOS) in the ferromagnetic electrodes. The spin asymmetry of DOS gives rise to a difference in currents between parallel (P) and antiparallel (AP) orientations of the electrode magnetizations and results in the tunnel magnetoresistance (TMR).[3–5] It follows from this model that the interfacial electronic structure should be an important factor in TMR.[6–9] To test this idea, attempts have been made to alter the interfacial electronic structure by introducing nonmagnetic (NM) metallic interlayers into the junction.[10–13] The observed TMR ratios[10–13] of such FM/I/NM/FM junctions showed an almost monotonic decrease with increasing thickness of the inserted layers of Au, Cu, or Cr. Zhang and Levy[14] have explained this decrease of TMR in terms of the decoherence of electrons propagating across a nonmagnetic layer.

The apparent agreement between the theory[14] and the early experiments on the junctions with nonmagnetic interlayers has been challenged by the recent observation of TMR in high-quality NiFe/Al_2O_3/Cu/Co junctions in which the Cu/Co electrode is a single crystal.[15] These experiments show clear oscillations of the TMR as function of Cu thickness. Two characteristic features of the oscillations have been observed: (i) the average TMR decays to zero with increasing Cu thickness; (ii) the period of oscillations is determined solely by the extremal wave vector k_F at the Cu Fermi surface (FS) belly. This is the same period that has been observed in the photoemission spectra[16] and oscillatory exchange coupling (Ref. 17 and references therein). The experiments of Yuasa *et al.*[15] pose some very fundamental questions concerning the effect of a nonmagnetic metallic interlayer on TMR. The fact that nonzero TMR has been observed for a thick spacer layer is the first clear evidence of coherent tunneling across the whole junction. This cannot be understood within the classical theory[3,4] which would predict strictly zero TMR. Nonzero TMR can be explained within the Kubo formalism applied to a junction with a vacuum gap[18] but the two principal features of the observed oscillations listed above cannot be understood within the existing theories.

The properties of conductance and TMR oscillations observed in epitaxial FM/I/Cu/FM junctions are quite different from those studied theoretically for metallic traylayers in the ballistic limit.[19,20] First, in contrast to the observed single period of oscillation, multiple oscillation periods have been predicted for metallic junctions. In addition to FS periods (k_F), the theory predicts also periods (k_{cp}) arising from a sudden cutoff of the conductance which occurs when the component of the electron energy perpendicular to the layers falls below the edge of a quantum well (QW) formed in the NM layer. The theoretical results on TMR in FM/I/Cu/FM junctions with a vacuum gap[18] also predict multiple oscillation periods. Second, the theory for FM/vacuum/Cu/FM junction fails completely to explain the observed oscillation of TMR about a zero average value.

The purpose of this work is to give a theoretical explanation for the characteristic features of the observed oscillation in TMR,[15] especially, the reasons for vanishing the average TMR and selection of k_F oscillation period. To achieve the purpose, we include disorder[21–29] in our calculation since diffusive scattering is disregarded in previous theories.[18,30] We calculate the spin-dependent conductance and the TMR ratio by applying the linear response theory and the single-

site coherent potential approximation (CPA) to a simple tight-binding model.

In this paper we show that the diffusive scattering (vertex correction) is decisive for the transport properties in tunneling junctions containing quantum well and that the combined effects of barrier thickness and disorder can explain all the essential features of experimental results. In particular, we will demonstrate that (i) increasing barrier thickness and disorder in the barrier increases the amplitude of the k_F oscillation period relative to the k_{cp} period, and (ii) the disorder in the barrier decreases the asymptotic value of the TMR ratio to zero. We further show that the calculated results can be reproduced by the stationary phase approximation,[20] which implies that this technique is applicable to a realistic multiorbital model of the tunneling junction. This clearly shows that the spanning vector k_F of the Cu FS is responsible for the observed oscillation period. In addition, we show that the amplitude of the oscillation becomes small with decreasing mean free path of the spacer.

This paper is organized as follows. In Sec. II, a simple tight-binding model for ferromagnetic tunneling junctions containing a quantum well is presented. Then, a formulation of the conductance within a framework of the Kubo formula and the single-site CPA with the vertex correction is given. In Sec. III, numerical results obtained for both clean and disordered junctions are shown and the effect of the disorder on the quantum oscillation of TMR is clarified. Finally we summarize this paper in Sec. IV.

II. MODEL AND METHOD

A. Model

Let us consider a FM/*I*/NM/FM junction on a simple cubic lattice with lattice spacing a, where FM, *I*, and NM denote a ferromagnetic electrode, an insulating barrier, and a nonmagnetic metallic spacer, respectively (see Fig. 1). We choose (001) axis (z axis) as a stacking direction and use $(\mathbf{r}_\parallel, l)$ representation where $\mathbf{r}_\parallel$ is a positional vector in x-y direction and l labels the layer in z direction. Initially we adopt a single-orbital tight-binding Hamiltonian in order to model a $Co/Al_2O_3/Cu/Co$ junction (analogous to $NiFe/Al_2O_3/Cu/Co$ junction studied in Ref. 15):

$$\hat{H} = \hat{W} + \hat{V} \tag{1}$$

$$\hat{W} = -t \sum_{\langle(\mathbf{r}_\parallel, l),(\mathbf{r}'_\parallel, l')\rangle, \sigma} (c^\dagger_{\mathbf{r}_\parallel, l, \sigma} c_{\mathbf{r}'_\parallel, l', \sigma} + \text{H.c.}), \tag{2}$$

$$\hat{V} = \sum_{\mathbf{r}_\parallel, l, \sigma} V^{\mathbf{r}_\parallel}_{l,\sigma} c^\dagger_{\mathbf{r}_\parallel, l, \sigma} c_{\mathbf{r}_\parallel, l, \sigma}, \tag{3}$$

where $c_{\mathbf{r}_\parallel, l, \sigma}$ ($c^\dagger_{\mathbf{r}_\parallel, l, \sigma}$) is the annihilation (creation) operator of an electron with spin $\sigma(=\uparrow,\downarrow)$ at site $(\mathbf{r}_\parallel, l)$, t the hopping integral between nearest-neighbor sites, and $V^{\mathbf{r}_\parallel}_{l,\sigma}$ the on-site potential for an electron with spin σ at site $(\mathbf{r}_\parallel, l)$.

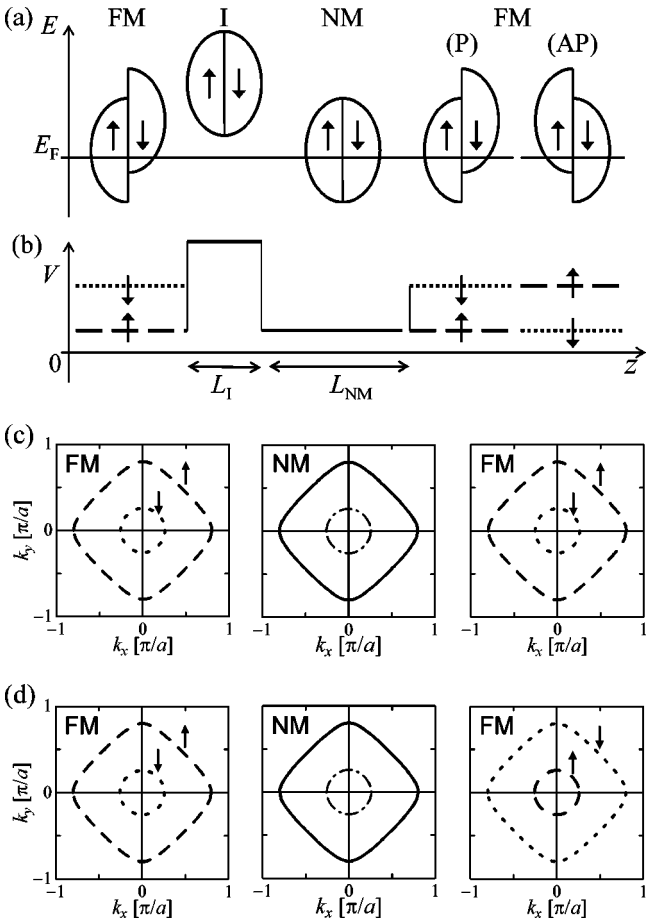

FIG. 1. (Color online) Schematic representation of DOS (a), potential profile (b), and projected Fermi surface (FS) in *P* (c) and AP (d) alignments of a FM/*I*/NM/FM junction. In AP alignment, the magnetization of right FM is opposite to that of left FM. In (b), on-site potentials for ↑ and ↓ spins are shown by dashed and dotted lines, respectively. In (c) and (d), projected FS of ↑ and ↓ spin states in FM are regions inside of dashed and dotted loops, respectively. NM FS is shown by solid loop and dash-dotted circles in NM FS of (c) and (d) give the cutoff wave vector k_{cp} for ↓ and ↑ spin states, respectively.

Here, we chose the magnetization direction of left FM as the global spin quantization axis. In *P* (AP) alignment, the magnetization of right FM is parallel (antiparallel) to that of left FM. Since the majority spin band of Co is similar to the Cu band, we set in the left FM $V_{FM\uparrow} = V_{NM}$. The potential profile of the system and the FS projected onto k_x-k_y plane for both *P* and AP alignments are shown in Figs. 1(b), 1(c), and 1(d), respectively, where $\mathbf{k}_\parallel = (k_x, k_y)$ is the element of the wave vector parallel to the x-y plane, or the lateral direction. It is clear that quantum well states are formed in NM layer only for ↓-spin electrons in *P* alignment and ↑-spin electrons in AP alignment. Since the insulating Al_2O_3 barrier is amorphous in real junctions, we introduce disorder in the barrier by setting $V^{\mathbf{r}_\parallel}_{l,\sigma} = V_I + \Delta V_I$ or $V_I - \Delta V_I$ randomly depending on the site in equal probabilities. We also introduce disorder in NM by setting $V^{\mathbf{r}_\parallel}_{l,\sigma} = V_{NM} + \Delta V_{NM}$ or $V_{NM} - \Delta V_{NM}$. Altogether, the on-site potential is

$$V(\mathbf{r}_\parallel,l)=\begin{cases} V_{\mathrm{FM}}^{\sigma}, & l\in \text{left FM} \\ V_{\mathrm{I}}\pm\Delta V_{\mathrm{I}}, & l\in I \\ V_{\mathrm{NM}}\pm\Delta V_{\mathrm{NM}}, & l\in \mathrm{NM} \\ V_{\mathrm{FM}}^{\sigma(\bar{\sigma})}, & l\in \text{right FM in } P(\mathrm{AP}). \end{cases} \tag{4}$$

The tunneling conductance for σ-spin electron in P (AP) alignment is given by

$$G_{\mathrm{P(AP)}}^{\sigma}=\frac{e^2}{h}\sum_{\mathbf{k}_\parallel,\mathbf{k}'_\parallel} t_{\mathrm{P(AP)}}^{\sigma}(\mathbf{k}_\parallel\rightarrow\mathbf{k}'_\parallel), \tag{5}$$

where $t_{\mathrm{P(AP)}}^{\sigma}(\mathbf{k}_\parallel\rightarrow\mathbf{k}'_\parallel)$ is the transmission coefficient for an electron incident from the left FM with $\mathbf{k}_\parallel$ and scattered into the right FM with $\mathbf{k}'_\parallel$. TMR ratio is defined by $\mathrm{TMR}\equiv 1-(G_{\mathrm{AP}}^{\uparrow}+G_{\mathrm{AP}}^{\downarrow})/(G_{\mathrm{P}}^{\uparrow}+G_{\mathrm{P}}^{\downarrow})$.

B. Formulation of the conductance

In this subsection, we formulate the electrical conductance for layered system including disorder mentioned in preceding subsection by using the linear response theory and the CPA.

In the Kubo formula,[31] the conductance is expressed by current-current correlation functions. Conductance G for the currents perpendicular to the layers (z direction) per spin channel is given as[32]

$$G=\frac{\pi\hbar}{(2\pi a i)^2}\langle \mathrm{Tr}[\hat{J}_z(m)[\hat{g}(z_-)-\hat{g}(z_+)] \times\hat{J}_z(n)[\hat{g}(z_-)-\hat{g}(z_+)]]\rangle, \tag{6}$$

where the bracket $\langle\cdots\rangle$ denotes the configurational average of the quantity "$\cdots$" over the disorder. We omit the spin index σ for simplicity in this subsection. The local current operator $\hat{J}_z(l)$ in the z direction and the Green's function $\hat{g}(z)$ are given by

$$\hat{J}_z(l)=\frac{ieta}{\hbar}\sum_{\mathbf{r}_\parallel}(c^{\dagger}_{\mathbf{r}_\parallel,l+1}c_{\mathbf{r}_\parallel,l}-c^{\dagger}_{\mathbf{r}_\parallel,l}c_{\mathbf{r}_\parallel,l+1}), \tag{7}$$

$$\hat{g}(z_\pm)=(z_\pm\mathbb{1}-\hat{H})^{-1},\quad (z_\pm=E_{\mathrm{F}}\pm i0), \tag{8}$$

where E_{F} is the Fermi energy.

In order to calculate the conductance, we need to evaluate the configurational average of the product of two Green's functions such as $\langle\hat{J}_z(m)\hat{g}(z_1)\hat{J}_z(n)\hat{g}(z_2)\rangle$.

The configurational average can be evaluated by several methods, for example, numerical simulation and mean-field approximation. In the numerical simulation, the conductance is calculated for a cluster whose size is finite in lateral direction.[24] The average value of the conductance is obtained by statistical averaging over clusters which have different configuration of disorder. The formulation is straightforward and the conductance is expressed in terms of fully real-space Green's functions which can be obtained numerically by using the recursion method.[32]

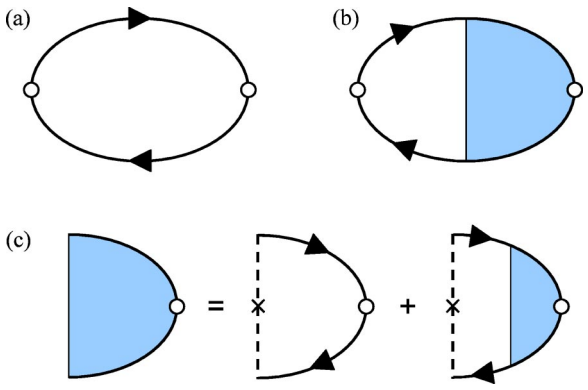

FIG. 2. (Color online) Feynman diagrams for conductance. (a) and (b) denote the first and second terms of right-hand side of Eq. (9), respectively. (c) represents the ladder approximation for the vertex function in Eq. (15). Solid line with an arrow, dashed line, open circle, and shaded area are the effective Green's function, the single-site t matrix, the local current operator, and the vertex function, respectively.

In the mean-field approximation, the configurational average of the product of two Green's functions is divided into two parts as (see Fig. 2)

$$\begin{aligned}\langle\hat{J}_z(m)\hat{G}(z_1)\hat{J}_z(n)\hat{G}(z_2)\rangle &=\hat{J}_z(m)\hat{\mathcal{G}}(z_1)\hat{J}_z(n)\hat{\mathcal{G}}(z_2)\\ &\quad+\hat{J}_z(m)\hat{\mathcal{G}}(z_1)\hat{\Lambda}(z_1,\hat{J}_z(n),z_2)\hat{\mathcal{G}}(z_2).\end{aligned} \tag{9}$$

The first term is the product of the two effective Green's functions which include the effective media, or self-energy. The second term is the vertex correction which should be estimated consistently with the self-energy to satisfy the current conservation law. In simple alloy systems, the vertex correction vanishes due to the symmetry of the system. However, in tunneling junctions, the correction does not vanish because of the layered structure of the system and describes diffusive scattering processes where electron momentum along layers is not conserved.

We adopt the single-site CPA (Ref. 33) as a mean-field approximation and outline below how the effective Green's function $\hat{\mathcal{G}}(z)$ and the vertex function $\hat{\Lambda}(z_1,\hat{J}_z(n),z_2)$ are determined.[24] In the CPA, the effective Green's function is obtained by replacing random potential $\hat{V}$ with an effective media,[33]

$$\hat{\mathcal{G}}(z)=[z\mathbb{1}-\hat{W}-\hat{\Sigma}(z)]^{-1}. \tag{10}$$

where $\hat{\Sigma}(z)$ is the coherent potential. In the single-site approximation, the coherent potential becomes site diagonal and depends on the layer index in a layered system,

$$\hat{\Sigma}(z)=\sum_{\mathbf{r}_\parallel,l}\Sigma_l(z)c^{\dagger}_{\mathbf{r}_\parallel,l}c_{\mathbf{r}_\parallel,l}. \tag{11}$$

The potential $\Sigma_l(z)$ is determined so that the average of the single-site t matrix vanishes, i.e.,

$$\langle \tau_l^{\mathbf{r}_\parallel}(z)\rangle = 0, \tag{12}$$

$$\tau_l^{\mathbf{r}_\parallel}(z) \equiv [V_l^{\mathbf{r}_\parallel} - \Sigma_l(z)]\{1 - \mathcal{G}_{ll}^{\mathbf{r}_\parallel \mathbf{r}_\parallel}(z)[V_l^{\mathbf{r}_\parallel} - \Sigma_l(z)]\}^{-1}. \tag{13}$$

Here, since $\hat{\Sigma}$, then, $\hat{\mathcal{G}}$ has the translational invariance in the x-y directions, $\mathcal{G}_{ll'}^{\mathbf{r}_\parallel \mathbf{r}'_\parallel}$ is rewritten in $(\mathbf{k}_\parallel, l)$ representation as

$$\mathcal{G}_{ll'}^{\mathbf{r}_\parallel \mathbf{r}'_\parallel}(z) = \frac{1}{N_{xy}} \sum_{\mathbf{k}_\parallel} e^{i\mathbf{k}_\parallel \cdot (\mathbf{r}_\parallel - \mathbf{r}'_\parallel)} \langle \mathbf{k}_\parallel, l | \{(z - W_{\mathbf{k}_\parallel})\mathbb{1} - \hat{\Sigma}(z)\}^{-1} | \mathbf{k}_\parallel, l' \rangle, \tag{14}$$

where $W_{\mathbf{k}_\parallel} = -2t[\cos(k_x a) + \cos(k_y a)]$. The coherent potential is a complex number at layers with disorder reflecting the effect of scatterings whereas it is the only on-site potential at layers without disorder. Therefore, by solving self-consistent equations (12)–(14), we can obtain $\Sigma_l(z)$ and the effective Green's function as long as the number of disordered layers is finite.

Next we evaluate the vertex correction term in Eq. (9). The vertex correction should be calculated consistently with the coherent potential (self-energy) in order to satisfy the current conservation law. We apply the ladder approximation and calculate Feynman diagrams in Fig. 2(c). In this approximation, the vertex function becomes site diagonal as $\hat{\Lambda} = \Sigma_{\mathbf{r}_\parallel, l} \Lambda_l c^\dagger_{\mathbf{r}_\parallel, l} c_{\mathbf{r}_\parallel, l}$ and Λ_l satisfies the following equation:[34]

$$\Lambda_l(z_1, \hat{J}_z(n), z_2) = \langle \tau_l^{\mathbf{r}_\parallel}(z_1)\, \tau_l^{\mathbf{r}_\parallel}(z_2)\rangle \left\{ \mathcal{K}_{ll}^{\mathbf{r}_\parallel \mathbf{r}_\parallel}[z_1, \hat{J}_z(n), z_2] + \sum_{\substack{(\mathbf{r}'_\parallel, l') \\ \neq (\mathbf{r}_\parallel, l)}} \mathcal{G}_{ll'}^{\mathbf{r}_\parallel \mathbf{r}'_\parallel}(z_1) \Lambda_{l'}(z_1, \hat{J}_z(n), z_2) \mathcal{G}_{l'l}^{\mathbf{r}'_\parallel \mathbf{r}_\parallel}(z_2) \right\}, \tag{15}$$

$$\mathcal{K}_{ll}^{\mathbf{r}_\parallel \mathbf{r}_\parallel}[z_1, \hat{J}_z(n), z_2] = \{\hat{\mathcal{G}}(z_1) \hat{J}_z(n) \hat{\mathcal{G}}(z_2)\}_{ll}^{\mathbf{r}_\parallel \mathbf{r}_\parallel}. \tag{16}$$

Equation (15) is a simultaneous equation for Λ_l, which can be solved since Λ_l is nonzero only at layers with disorder.

In the present formalism, the conductance is expressed by quantities which recover the translational invariance in lateral direction. Therefore, mixed $(\mathbf{k}_\parallel, l)$ representation is used in the calculation. The procedure to calculate the conductance is summarized as follows. We first calculate the layer-dependent coherent potentials $\{\Sigma_l\}$ by solving Eqs. (12)–(14). Once the coherent potentials are determined, any matrix elements of the effective Green's function in Eq. (14) can be easily calculated because the effective Green's function is $\mathbf{k}_\parallel$ diagonal.[24] We use the recursion method[32] for the calculation. The surface Green's function of electrodes, which is required for the method, is given in an analytic way[35] in our simple model. Next, we calculate the layer-dependent vertex functions $\{\Gamma_l\}$ by solving Eqs. (15) and (16). Then we calculate the conductance by using Eqs. (6) and (9).

Because of the current conservation law, the layer indices m and n of local current operators in Eq. (6) are arbitrary. We have confirmed that the conductance does not depend on the choice of m and n in our calculation. When we take m and n surface layers of left and right leads, respectively, the expression for conductance is reduced to Eq. (5).[36]

In order to confirm the results obtained by the CPA, we have also performed numerical simulations[23] for finite-size clusters. In the numerical simulations, a 24×24 sites supercell with 32×32 supercell $\mathbf{k}_\parallel$ points in two-dimensional Brillouin zone was used. The results obtained by the CPA and the numerical simulation agree satisfactorily. The CPA calculation, however, has advantages over the numerical simulation in computational time and memory.

The method of the single site CPA with the vertex correction has been applied to metallic multilayers,[37] ordinal tunneling junctions,[24] and also tunneling junctions containing manganites.[38] It has been shown that the method is applicable even to rather strongly disordered systems,[39] although the single site CPA neglects the correlation between scatterings.

III. RESULTS

In our numerical calculations, we use in the left FM $V_{\mathrm{FM}\uparrow} = V_{\mathrm{NM}} = 2.382t$ and $V_{\mathrm{FM}\downarrow} = 5.382t$. The barrier potential and and the Fermi energy are set as $V_{\mathrm{I}} = 9.0t$ and $E_{\mathrm{F}} = 0$, respectively. The barrier thickness is five atomic layers unless specified. Such a choice of parameters reproduces approximately the observed TMR ratio for a junction without the nonmagnetic spacer and the oscillation period originating from Cu FS belly.

We show calculated results for clean junctions ($\Delta V_{\mathrm{I}} = \Delta V_{\mathrm{NM}} = 0$), junctions with disorder in the insulating barrier ($\Delta V_{\mathrm{I}} \neq 0, \Delta V_{\mathrm{NM}} = 0$), and junctions with disorder in both the barrier and the spacer ($\Delta V_{\mathrm{I}} \neq 0, \Delta V_{\mathrm{NM}} \neq 0$) in Secs. III A, III B, and III C, respectively.

A. TMR in clean junctions

First, the spin-dependent conductances and TMR ratios of junctions without disorder ($\Delta V_{\mathrm{I}} = \Delta V_{\mathrm{NM}} = 0$) are shown in Figs. 3(a) and 3(b), respectively. It can be seen that $G_{\mathrm{P}}^{\downarrow}$ and $G_{\mathrm{AP}}^{\uparrow}$ oscillate with the NM layer thickness L_{NM} due to interference of electrons in the spacer quantum well. The oscillations are a superposition of two periods: the FS period determined by the Fermi wave vector k_{F} and a period given by the cutoff wave vector k_{cp}. The Fermi wave vector, which originates from the state with $\mathbf{k}_\parallel = 0$, is given by $2t\cos(k_{\mathrm{F}} a) = V_{\mathrm{NM}} - E_{\mathrm{F}} - 4t$. The cutoff period originates from sudden cutoff of the conductance at $\mathbf{k}_\parallel$ points shown by dash-dotted curve in NM FS of Figs. 1(c) and 1(d), and the cutoff wave vector is given by $2t\cos(k_{\mathrm{cp}} a) = V_{\mathrm{NM}} - V_{\mathrm{FM}\downarrow} + 2t$.[19]

For the potential parameters chosen, the FS and cutoff periods, corresponding to $k_{\mathrm{F}} = 4\pi/5a$ and $k_{\mathrm{cp}} = 2\pi/3a$, are $5a$ and $3a$. The situation here is analogous to that of CPP-

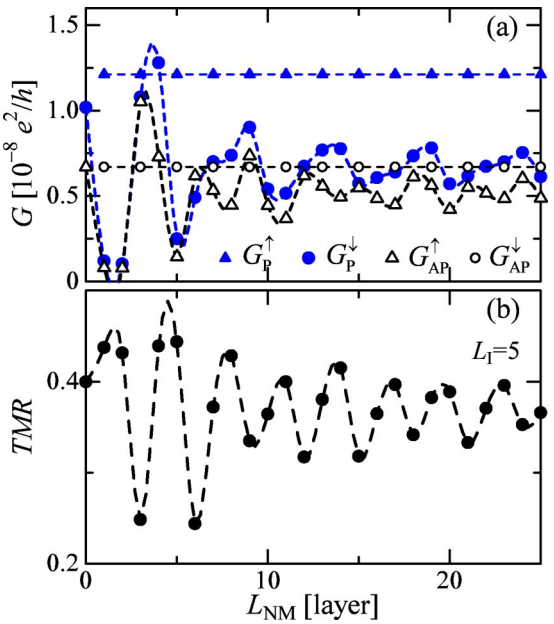

FIG. 3. (Color online) Conductance (a) and TMR ratio (b) of clean junctions. Conductances for ↑ and ↓ spin electrons are denoted by ▲ (△) and ● (○), respectively, for *P* (AP) alignment of magnetizations. Dashed lines are guide to the eye.

GMR in a Co/Cu/Co trilayer.[20] The TMR ratio shown in Fig. 3(b) oscillates with the same periods as the conductance and has a finite asymptotic value for large NM thicknesses. These results are consistent with those of Ref. 18 where the effect of disorder was ignored.

Figure 4 shows the dependence of oscillations in $G_P^{\downarrow}$ and $G_{AP}^{\uparrow}$ on the barrier thickness L_I with all the conductances being normalized to the asymptotic values $G_P^{\downarrow\infty}$ and $G_{AP}^{\uparrow\infty}$ for $L_{NM}\to\infty$, respectively. The oscillation period of $G_P^{\downarrow}$ clearly tends to $5a$ with increasing barrier thickness. This result is explained as follows. Since the wave vector $\mathbf{k}_\parallel$ parallel to the interface is conserved in the system without disorder, the transmission probability $T^{\sigma}_{P(AP)}(\mathbf{k}_\parallel)$ for an electron incident from the left FM with momentum $\mathbf{k}_\parallel$ on the barrier is given as $T^{\sigma}_{P(AP)}(\mathbf{k}_\parallel)=t^{\sigma}_{P(AP)}(\mathbf{k}_\parallel\to\mathbf{k}_\parallel)$. In Fig. 5, the transmission probabilities are plotted as functions of $\mathbf{k}_\parallel$ in a logarithmic scale. Here, $T_P^{\uparrow}$ takes a finite value in wider range of $\mathbf{k}_\parallel$ plane than the others because of large FM FS of ↑-spin electron and the momentum conservation. The transmission probability depends strongly on the angle of incidence of electrons on the barrier, and the normal incidence [$\mathbf{k}_\parallel=(0,0)$] contributes most to the conductance. It follows that, as the barrier thickness increases, the oscillation due to cutoff k points, i.e., $\mathbf{k}_\parallel\neq(0,0)$, becomes progressively weakened compared to that of the FS oscillation, i.e., $\mathbf{k}_\parallel=(0,0)$. For $G_{AP}^{\uparrow}$, the increase in oscillation period from $3a$ to $5a$ is only seen for larger L_I. This may be due to the fact that $T_{AP}^{\uparrow}[\mathbf{k}_\parallel=(0,0)]/\Sigma_{\mathbf{k}_\parallel}T_{AP}^{\uparrow}(\mathbf{k}_\parallel)$ is smaller than $T_P^{\downarrow}[\mathbf{k}_\parallel=(0,0)]/\Sigma_{\mathbf{k}_\parallel}T_P^{\downarrow}(\mathbf{k}_\parallel)$, i.e., the contribution of normal incidence to the conductance $G_{AP}^{\uparrow}$ is smaller than that to $G_P^{\downarrow}$. As a result, the oscillation period of the TMR ratio is not quite $5a$ for the present barrier thickness.

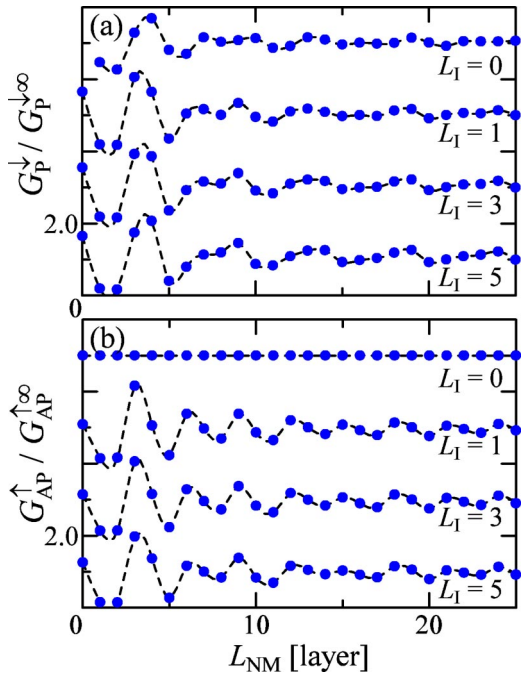

FIG. 4. (Color online) Conductance $G_P^{\downarrow}$ for various thicknesses of clean insulating barrier normalized to the asymptotic value obtained at $L_{NM}\to\infty$. Dashed lines are guides to the eye.

B. TMR in disordered junctions

Next, we introduce disorder into the insulating barrier ($\Delta V_I=0.5t, \Delta V_{NM}=0$) and show the corresponding calculated results of spin-dependent conductance and TMR ratio in Figs. 6(a) and 6(b). The conductance $G_{AP}^{\uparrow}$ is clearly enhanced by disorder whereas all the other conductances $G_P^{\uparrow}$, $G_P^{\downarrow}$, and $G_{AP}^{\downarrow}$ are hardly affected. $G_{AP}^{\uparrow}$ now oscillates almost exclusively with period $5a$ (i.e., k_F period) about $G_P^{\uparrow}$ [see Fig. 6(a)]. This results in a TMR ratio which now oscillates around zero with the period $5a$. This should be contrasted with the ordered case in which the TMR ratio oscillates with two periods about a constant background [cf. Fig. 6(b) and Fig. 3(b)]. The asymptotic values of the TMR ratio as $L_{NM}\to\infty$ are shown in the inset of Fig. 6(b) as functions of the barrier thickness. Both the cases with and without disorder are shown. The asymptotic value of the TMR ratio for junctions without disorder decreases slowly with increasing L_I, whereas that for junctions with disorder decreases rapidly and becomes zero for large L_I.

To gain a better understanding of the effects of disorder on the magnitude of $G_{AP}^{\uparrow}$, and on the period of oscillations, we have calculated the dependence of the transmission probability on $\mathbf{k}_\parallel$. Figure 7 shows the transmission probabilities $T^{\sigma}_{P(AP)}(\mathbf{k}_\parallel)$ for an electron incident from the left FM with momentum $\mathbf{k}_\parallel$ on the barrier. In disordered junctions, since $\mathbf{k}_\parallel$ is not necessarily conserved, $T^{\sigma}_{P(AP)}(\mathbf{k}_\parallel)$ is given as $T^{\sigma}_{P(AP)}(\mathbf{k}_\parallel)\equiv\Sigma_{\mathbf{k}_\parallel'}t^{\sigma}_{P(AP)}(\mathbf{k}_\parallel\to\mathbf{k}_\parallel')$. In the absence of disorder, the contribution to $T_{AP}^{\uparrow}$ in the momentum space is concentrated near $\mathbf{k}_\parallel=(0,0)$ as shown in Fig. 5(c). However, disor-

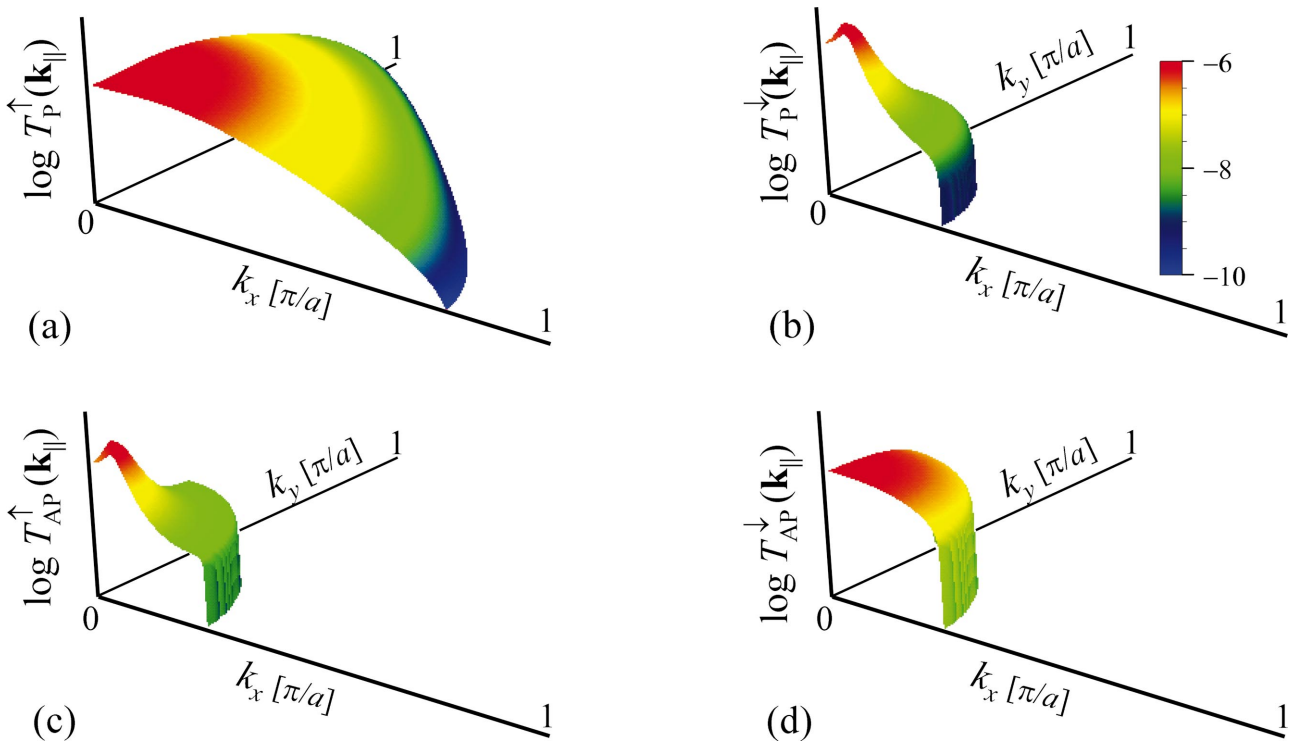

FIG. 5. (Color) $\mathbf{k}_\parallel$ dependence of transmission probabilities for clean junctions. Transmission probabilities of ↑ and ↓ spin electrons incident from left FM with $\mathbf{k}_\parallel$ are plotted in (a) and (b) for *P* alignment, and (c) and (d) for AP alignment.

der opens up additional channels $\mathbf{k}_\parallel$ outside this area contributing to $T_{AP}^{\uparrow}$ in Fig. 7(c). This is because $\mathbf{k}_\parallel$ is not conserved in diffusive scattering. In the absence of disorder, only $\mathbf{k}_\parallel$ points on the FS satisfying the $\mathbf{k}_\parallel$ conservation contribute to the conductance. For diffusive scattering, on the other hand, the entire set of $\mathbf{k}_\parallel$ points on the FS contributes to transport. More precisely, $\mathbf{k}_\parallel$ points corresponding to quantum well states contribute now to the conductance. These $\mathbf{k}_\parallel$ points appear as sharp peaks in Fig. 7(c) and they fall on concentric rings in the $\mathbf{k}_\parallel$ space.

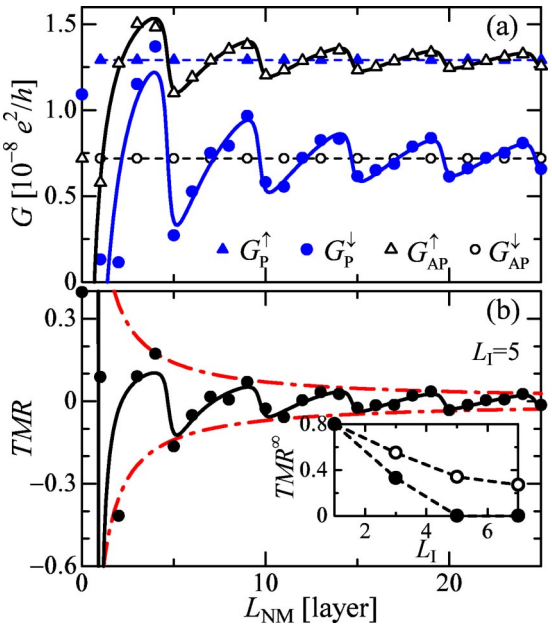

FIG. 6. (Color online) Conductance (a) and TMR ratio (b) of disordered junctions. Notation is same as in Fig. 2. Solid lines are obtained by the stationary phase approximation. Dash-dotted curves in (b) denote $1/L_{NM}$ dependence. Inset of (b): Asymptotic values of TMR ratio obtained at $L_{NM}\to\infty$ for clean (○) and disordered (●) junctions.

It is clear from Fig. 7(c), and examination of the ↑-spin FM FS, that the number of open $\mathbf{k}_\parallel$ channels contributing to $T_{AP}^{\uparrow}$, is now the same as that contributing to $T_P^{\uparrow}$. This explains the increase in the constant part of the conductance $G_{AP}^{\uparrow}$ to a value of approximately $G_P^{\uparrow}$. In addition, the introduction of diffusive scattering has almost eliminated the sharp momentum cut off seen in Fig. 7(c), which explains why the k_{cp} oscillation period of $G_{AP}^{\uparrow}$ is weakened by disorder. The other transmission probabilities are not greatly affected by the introduction of disorder [Figs. 7(a), 7(b), and 7(d)] since scattering cannot open new $\mathbf{k}_\parallel$ channels in these cases. This explains why the introduction of disorder has negligible effect on the conductances $G_P^{\uparrow}$, $G_P^{\downarrow}$, and $G_{AP}^{\downarrow}$. It is worth noting that the vertex correction is decisive for the transport properties in tunneling junctions containing a quantum well since most of the change in $G_{AP}^{\uparrow}$ and TMR ratio is brought about by the vertex correction.

We therefore expect that in the presence of disorder, the oscillatory part of the conductance is derived entirely from states in the region of $\mathbf{k}_\parallel=(0,0)$. In order to check this hypothesis, we have used the stationary phase method (see Ref. 20 and references therein), which is able to determine the oscillatory contributions from isolated regions of the Brillouin zone, for thick spacers. The results, depicted by solid curves in Figs. 6(a) and 6(b), are in excellent agreement with

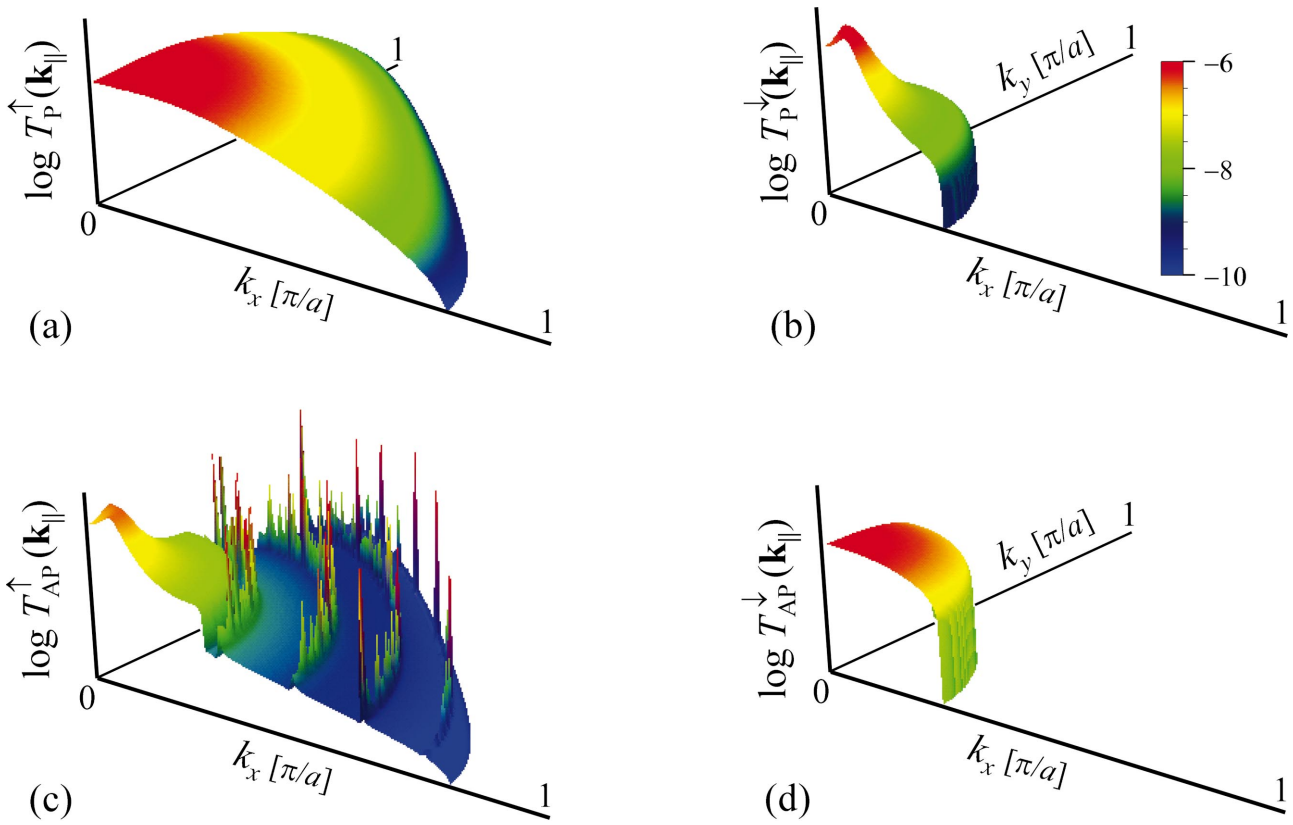

FIG. 7. (Color) $\mathbf{k}_\parallel$ dependence of transmission probabilities for disordered junctions. Transmission probabilities of ↑ and ↓ spin electrons incident from left FM with $\mathbf{k}_\parallel$ are plotted in (a) and (b) for *P* alignment, and (c) and (d) for AP alignment.

the numerical calculations for $L_{\mathrm{NM}} \gtrsim 5$. This indicates that the oscillation period observed in the experiment may be determined in the stationary phase approximation for a fully realistic model of the junction. The experimental finding[15] that the oscillation period is determined by k_{F} of the Cu spacer FS is thus naturally explained.

The physical interpretation of our results is as follows. The observed vanishing average of the TMR ratio is explained by disorder in the barrier which opens up new $\mathbf{k}_\parallel$ channels in the conductance of ↑-spin electrons in AP alignment. The number of open channels for ↑-spin electrons coming from a large FS of the left magnetic electrode is restricted, by the conservation of $\mathbf{k}_\parallel$ in the ordered junction, to the number of available channels on the FS of the right electrode, which is small since its relevant ↓ FS is small. Hence a spin asymmetry in transmission between *P* and AP alignments in the ordered junction arises. In a disordered junction, this restriction is removed and all the states from the large FS of the left electrode can now be scattered into the small FS of the right electrode. Hence the spin asymmetry is removed, and with it the average TMR. (Simple arguments along these lines show that the other transmission probabilities are not so affected by disorder.)

The selection of a single oscillation period (among many possible) is due to two factors. Periods corresponding to sharp cutoffs occur in an ordered junction because of a mismatch between the sizes of the FS of the FM and NM layers. The sharp cutoffs are "softened" in a disordered junction (the same argument as above). Periods coming from extrema of the spacer FS at $\mathbf{k}_\parallel \neq (0,0)$ are removed because perpendicular tunneling $\mathbf{k}_\parallel = (0,0)$ is favored in real junctions (period selection by barrier thickness).

C. Amplitude of TMR oscillation

In the preceding subsection, we have shown that the stationary phase approximation may well explain the TMR ratio obtained for junctions with disorder in the barrier (see Fig. 6). We can see from the result that the amplitude of the oscillation is inversely proportional to L_{NM}.[20] The experimental results, however, indicate a much faster decrease in the oscillation amplitude.[15] We, therefore, introduce disorder in the NM layer as well as in the barrier ($\Delta V_{\mathrm{I}} = 0.5t, \Delta V_{\mathrm{NM}} \neq 0$) and study how the amplitude of TMR oscillation is affected by the scattering in the spacer. By changing the disorder potential ΔV_{NM}, we calculate the conductance for several values of mean-free path λ_{NM} in the spacer. We estimated the mean-free path simply as $\lambda_{\mathrm{NM}} = \hbar v_{\mathrm{F}}/(2\mathrm{Im}\Sigma_0)$ where v_{F} and Σ_0 are the Fermi velocity of bulk NM and the coherent potential in bulk NM, respectively.

In Fig. 8(a), we show calculated results of the conductance $G_{\mathrm{AP}}^{\uparrow}$ for several values of λ_{NM}. We can see that the conductance $G_{\mathrm{AP}}^{\uparrow}$ decreases, i.e., the resistance increases with decreasing λ_{NM}, and that the amplitude of the oscillation is suppressed. Since we change λ_{NM}, the resistance in the spacer changes. In the inset of Fig. 8(a), we plot the resistance $1/G_0$ of the NM layer itself which is estimated for the system NM electrode/disordered NM layer/NM electrode.

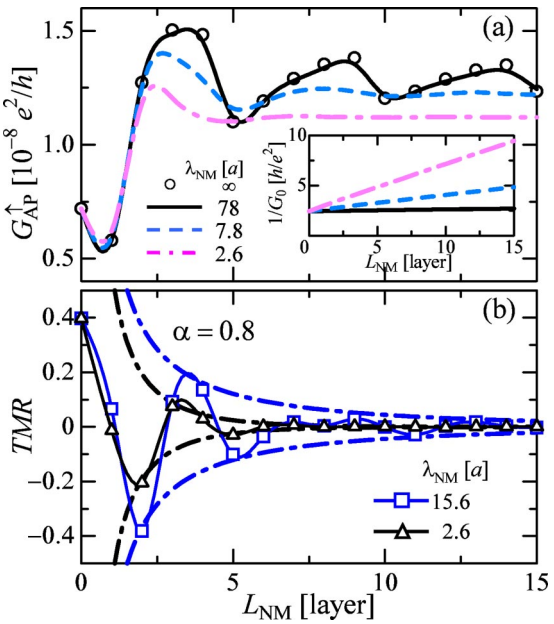

FIG. 8. (Color online) Conductance $G^{\uparrow}_{AP}$ (a) and TMR ratio (b). In (a), open circles, solid, dashed, and dash-dotted curves are results for $\lambda_{NM}=\infty$, $78a$, $7.8a$, and $2.6a$, respectively. In (b), open squares and triangles are results for $\lambda_{NM}=15.6a$ and $2.6a$, respectively. Dash-dotted curves denote $\pm\alpha/L_{NM}\exp(-L_{NM}/\lambda_{NM})$. Inset of (a): Resistance calculated for a system of NM electrode/disordered NM layer/NM electrode. Solid, dashed, and dash-dotted curves are results for $\lambda_{NM}=78a$, $7.8a$, and $2.6a$, respectively.

The resistance $1/G_0$ is too small to explain the change in the resistance $1/G^{\uparrow}_{AP}$ if we consider that the total resistance is given in series of the tunneling resistance and the spacer resistance. One explanation for large change in $G^{\uparrow}_{AP}$ could be that the disorder breaks quantum interference of the wave function caused by the quantum well at NM and makes the conductance smaller as compared with that with clean NM spacer. In Fig. 8(b), we show calculated results of the TMR ratio. It can be seen that the amplitude of the oscillation in the TMR ratio becomes small with decreasing λ_{NM} as well as that in the conductance. We found that the amplitude of the TMR oscillation can be described well by the form of $\alpha/L_{NM}\exp(-L_{NM}/\lambda_{NM})$ except for thin NM layer region. By fitting experimental data[15] using this expression, we estimated the mean-free path of Cu in the junction to be $\sim$20 Å, which is consistent with a theory based on the Boltzmann equation.[40]

IV. CONCLUSION

We have shown that the observed period of TMR oscillations and the oscillation of the TMR ratio around an averaged value close to zero are explained by the combined effects of tunneling barrier and disorder. Disorder introduces new conductance channels via quantum well states, which are confined at the nonmagnetic spacer in clean junctions. The new conduction channels increase the conductance of AP alignment to approximately that of *P* alignment, and average TMR ratio decreases to almost zero. Selection of perpendicular transmission due to the barrier and elimination of the sharp FS cutoff due to the disorder remove the cutoff oscillation period, and, only the FS period of the spacer remains.

Since the diffusive scattering caused by disorder is essential to explain experimental results, we can say that the vertex correction is decisive for the transport properties in tunneling junctions containing quantum well.

It has been also shown that the stationary phase approximation reproduces results obtained for junctions with disorder in the barrier quite well. The fact shows that the observed oscillation period in experiments can be explained in terms of the spanning vector k_F of the Cu spacer FS.

In addition, we have shown that disorder in the spacer breaks the interference occurred at the quantum well and suppresses the amplitude of the TMR oscillation. This is considered to be an origin of the rapid decrease in the amplitude of the TMR oscillation observed in experiments.[15]

We have used a rather simple tight-binding model in this paper since we intend to give qualitative explanation for the quantum oscillation of TMR. More realistic band calculations, however, showed that interfacial electronic structures, such as *p-d* bonding,[9,41] partially oxidized aluminum ion,[42,43] and hot-spot due to surface resonant states,[7,44,45] are important for TMR and the bias dependence. Stationary phase approximation enables to include both the more realistic electronic structures and the effect of disorder in calculations. Such fully realistic calculations of TMR are in progress.

ACKNOWLEDGMENTS

H.I. would like to thank JSPS and the CREST Suzuki team for valuable discussions and financial support. J.I. acknowledges the financial support of the NEDO International Joint Research Project (NAME).

[1] T. Miyazaki and N. Tezuka, J. Magn. Magn. Mater. **139**, L231 (1995).
[2] J.S. Moodera, L.R. Kinder, T.M. Wong, and R. Meservey, Phys. Rev. Lett. **74**, 3273 (1995).
[3] M. Julliere, Phys. Lett. **54A**, 225 (1975).
[4] S. Maekawa and U. Gäfvert, IEEE Trans. Magn. **18**, 707 (1982).
[5] J.C. Slonczewski, Phys. Rev. B **39**, 6995 (1989).
[6] J.M. MacLaren, X.-G. Zhang, T.C. Schulthess, and W.H. Butler, Phys. Rev. B **63**, 054416 (2001).
[7] J. Mathon and A. Umerski, Phys. Rev. B **63**, 220403 (2001).
[8] J.M. De Teresa, A. Barthélémy, A. Fert, J.P. Contour, R. Lyonnet, F. Montaigne, P. Seneor, and A. Vaurès, Phys. Rev. Lett. **82**, 4288 (1999).
[9] I.I. Oleinik, E.Yu. Tsymbal, and D.G. Pettifor, Phys. Rev. B **62**, 3952 (2001).
[10] J.S. Moodera, J. Nowak, L.R. Kinder, P.M. Tedrow, R.J.M. van de

Veerdonk, B.A. Smith, M. van Kampen, H.J.M. Swagten, and W.J.M. de Jonge, Phys. Rev. Lett. **83**, 3029 (1999).
[11] J.J. Sun and P.P. Freitas, J. Appl. Phys. **85**, 5264 (1999).
[12] P. LeClair, H.J.M. Swagten, J.T. Kohlhepp, R.J.M. van de Veerdonk, and W.J.M. de Jonge, Phys. Rev. Lett. **84**, 2933 (2000).
[13] P. LeClair, J.T. Kohlhepp, H.J.M. Swagten, and W.J.M. de Jonge, Phys. Rev. Lett. **86**, 1066 (2001).
[14] S. Zhang and P.M. Levy, Phys. Rev. Lett. **81**, 5660 (1998).
[15] S. Yuasa, T. Nagahama, and Y. Suzuki, Science **297**, 234 (2002).
[16] J.E. Ortega and F.J. Himpsel, Phys. Rev. Lett. **69**, 844 (1992).
[17] J. Mathon, M. Villeret, A. Umerski, R.B. Muniz, J. d'Albuquerque e Castro, and D.M. Edwards, Phys. Rev. B **56**, 11 797 (1997).
[18] J. Mathon and A. Umerski, Phys. Rev. B **60**, 1117 (1999).
[19] J. Mathon, M. Villeret, and H. Itoh, Phys. Rev. B **52**, R6983 (1995).
[20] J. Mathon, A. Umerski, and M. Villeret, Phys. Rev. B **55**, 14 378 (1997).
[21] A.M. Bratkovsky, Phys. Rev. B **56**, 2344 (1997).
[22] E.Yu. Tsymbal and D.G. Pettifor, Phys. Rev. B **58**, 432 (1998).
[23] H. Itoh, T. Kumazaki, J. Inoue, and S. Maekawa, Jpn. J. Appl. Phys. **37**, 5554 (1998).
[24] H. Itoh, A. Shibata, T. Kumazaki, J. Inoue, and S. Maekawa, J. Phys. Soc. Jpn. **69**, 1632 (1999).
[25] A. Vedyayev, D. Bagrets, A. Bagrets, and B. Dieny, Phys. Rev. B **63**, 064429 (2001).
[26] D. Bagrets, A. Bagrets, A. Vedyayev, and B. Dieny, Phys. Rev. B **65**, 064430 (2002).
[27] J. Inoue, N. Nishimura, and H. Itoh, Phys. Rev. B **65**, 104433 (2002).
[28] J. Inoue and H. Itoh, J. Phys. D **35**, 2437 (2002).
[29] E.Y. Tsymbal, O.N. Mryasov, and P.R. LeClair, J. Phys.: Condens. Matter **15**, R109 (2003).
[30] A. Vedyayev, N. Ryzhanova, C. Lacroix, L. Giacomoni, and B. Dieny, Europhys. Lett. **39**, 219 (1997).
[31] R. Kubo, J. Phys. Soc. Jpn. **17**, 975 (1957).
[32] P. Lee and D.S. Fisher, Phys. Rev. Lett. **47**, 882 (1981).
[33] P. Soven, Phys. Rev. **156**, 809 (1967).
[34] B. Velicky, Phys. Rev. **184**, 614 (1969).
[35] A.P. Sutton, M.W. Finnis, D.G. Pettifor, and Y. Ohta, J. Phys. C **21**, 35 (1988).
[36] C. Caroli, R. Combescot, P. Nozieres, and D. Saint-James, J. Phys. C **4**, 916 (1971).
[37] H. Itoh, J. Inoue, and S. Maekawa, Phys. Rev. B **51**, 342 (1995).
[38] H. Itoh, T. Ohsawa, and J. Inoue, Phys. Rev. Lett. **84**, 2501 (2000).
[39] H. Itoh, J. Inoue, S. Maekawa, and P. Bruno, J. Magn. Magn. Mater. **198-199**, 545 (1999).
[40] Y. Suzuki (private communication).
[41] E.Yu. Tsymbal, I.I. Oleinik, and D.G. Pettifor, J. Appl. Phys. **87**, 5230 (2000).
[42] H. Itoh and J. Inoue, Surf. Sci. **493**, 748 (2001).
[43] H. Itoh and J. Inoue, J. Magn. Magn. Mater. **226-230**, 930 (2001).
[44] J.M. MacLaren, X.-G. Zhang, W.H. Butler, and X. Wang, Phys. Rev. B **59**, 5470 (1999).
[45] O. Wunnicke, N. Papanikolaou, R. Zeller, P.H. Dederichs, V. Drchal, and J. Kudrnovský, Phys. Rev. B **65**, 064425 (2002).